



HAL
open science

Destruction analyses of power supplies due to electric pulse

G. Mejezaze, T. Dubois, L. Curos, F. Puybaret, J.-M. Vinassa

► **To cite this version:**

G. Mejezaze, T. Dubois, L. Curos, F. Puybaret, J.-M. Vinassa. Destruction analyses of power supplies due to electric pulse. *Microelectronics Reliability*, 2019, 100-101, pp.113470 -. 10.1016/j.microrel.2019.113470 . hal-03488481

HAL Id: hal-03488481

<https://hal.science/hal-03488481>

Submitted on 21 Dec 2021

HAL is a multi-disciplinary open access archive for the deposit and dissemination of scientific research documents, whether they are published or not. The documents may come from teaching and research institutions in France or abroad, or from public or private research centers.

L'archive ouverte pluridisciplinaire **HAL**, est destinée au dépôt et à la diffusion de documents scientifiques de niveau recherche, publiés ou non, émanant des établissements d'enseignement et de recherche français ou étrangers, des laboratoires publics ou privés.



Distributed under a Creative Commons Attribution - NonCommercial 4.0 International License

Destruction analyses of power supplies due to electric pulse

G. Mejecaze^{a,b,*}, T. Dubois^b, L. Curos^{a,b}, F. Puybaret^a, J.-M. Vinassa^b

^a CEA, DAM, CEA – Gramat, F-46500 Gramat, France

^b Univ. Bordeaux, CNRS, Bordeaux INP, IMS UMR 5218, 351 cours de la libération, F-33400 Talence, France

Abstract

This paper presents the effects of high amplitude conducted electromagnetic pulses on the electrical behaviour of a flyback switch-mode power supply. The electromagnetic pulse is injected using a Current Injection Platform (PIC, standing for “Plateforme d’Injection en Courant” in french) able to generate conducted electric pulses of several hundreds of amperes. Injections are performed in common mode and in differential mode until the power supply destruction. These destruction tests permit to show that common mode injection is more destructive than differential mode injection. Moreover, in most cases, it is shown that the same components are destroyed. Components analyses were performed and permit to make some hypotheses about their failure.

1. Introduction

With the growth of electronics and the emergence of microelectronics, electrical systems are increasingly susceptible regarding intentional electromagnetic interferences (IEMI) which are a real threat since late 1990s [1]. Moreover, with the spread of high-power electromagnetic (EM) pulse sources [2], a risk of intentional EM attack exists [3, 4] and so, it becomes important to study and understand the effects of such disturbances on the behaviour of electronic systems. The most powerful sources are generally pulse sources able to generate electric field of several kilo volts per meter potentially inducing irreversible degradation of the victim system.

In this domain, most of the studies found in the literature deal with the effects of electromagnetic pulse (EMP) on large systems [5] or integrated circuits such as microcontrollers and logic circuits [6]. Based on this state of the art, two observations can be done. Firstly, few studies deal with the effects of EMP on switch-mode power supplies (SMPS) [7]. However, when an EMP is radiated over buildings or houses, the EMP can couple to their electrical distribution network. The interference can propagate to the different electronic devices plugged to the grid and can disturb them [8]. Secondly, due to the system complexity, most of the time, only ascertainment of the electronic equipment destruction is done [7, 9]. Only few studies propose an analysis of the destruction effects at component level [4]. However, in order to understand and to explain the failure of the global system, an analysis of its components is necessary [10].

The aim of this paper is to present and analyse the failure of a flyback SMPS induced by high amplitude electromagnetic pulses through the analysis of its destroyed components. The chosen SMPS has been specially designed

after the studies of a wide range of commercial SMPS topologies and components in order that it is representative of a majority of commonly used power supplies.

The second part of the paper presents the experimental setup with the current pulse source used to generate SMPS failures in conducted mode. It also presents the schematic of the tested SMPS. In the third section, destruction results are shown with the most frequently broken components and the comparison between common mode and differential mode injections. Section four deals with the analysis results allowing to understand the failure causes. Finally, section five is dedicated to the conclusions.

2. Experimental setup and DUT

2.1. PIC

The Current Injection Platform (PIC, standing for “Plateforme d’Injection en Courant” in french), illustrated in Fig. 1, is a source able to generate a single current pulse of several hundreds of amperes and hundreds of nanoseconds duration.

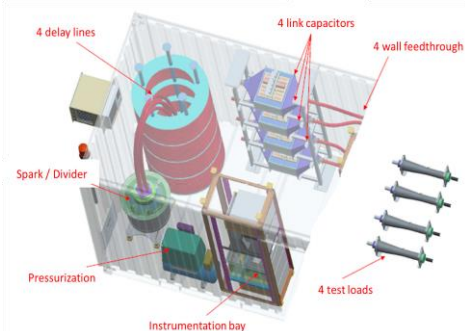


Fig. 1. Current Injection Platform (PIC).

* Corresponding author. guillaume.mejecaze@ims-bordeaux.fr
Tel: +33 (0)56 510 5481

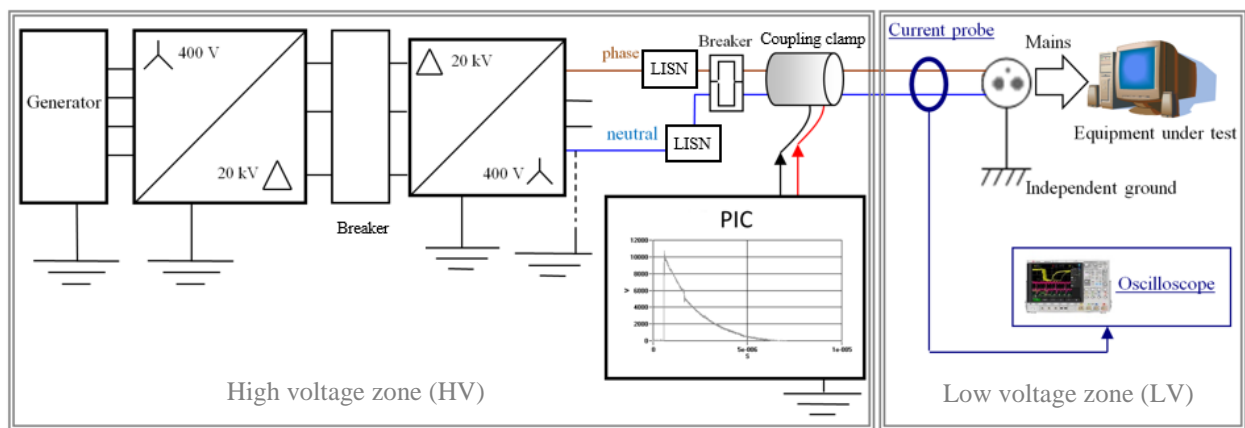


Fig. 2. The whole current injection source

It is described by Eq. (1) and illustrated in Fig. 3. PIC generates the coupling result of the wave described in the HEMP standard (High - Altitude Electromagnetic Pulse - IEC 61000-2-9 [11]) on distribution network long cables.

$$E(t) = k E_{01}(e^{-at} - e^{-bt}) \quad (1)$$

In Eq. (1) k , E_{01} , a and b are scalars.

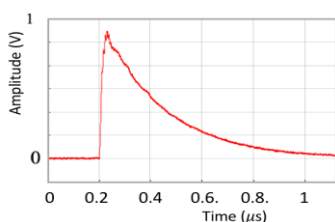


Fig. 3. Example of a bi-exponential shape.

PIC is associated to the electrical generation-transformation-distribution network presented in Fig. 2 allowing to power the equipment under test. This installation is totally autonomous and is representative of a conventional high voltage / low voltage (HV / LV) distribution. Then, the equipment under test is directly connected to the step-down transformer through Line Impedance Stabilization Network (LISN).

The differential / common mode injection is performed using inductive coupling clamp. As presented in Fig. 4, in differential mode, one wire (phase or neutral conductor) goes through the coupling clamp, and in common mode, the two wires (phase and neutral) go through the clamp.

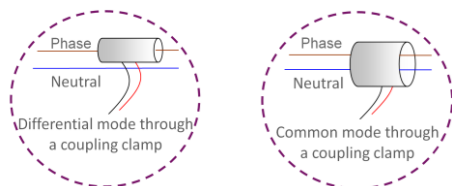


Fig. 4. Differential and common-modes injection.

In order to measure the injected current signal, current probes like 110A, 2100 or 8585C from Pearson manufacturer are used. Moreover, current and voltage signals during the injection can be measured directly at different points of the SMPS using CT2 current probe from Tektronix and high voltage differential probe like IsoVu from Tektronix or N2891A from Keysight.

2.2. Tested switch-mode power supply

2.2.1. Preliminary studies

In order to design a representative power supply for testing, a study of a wide range of commercial SMPS topologies and components has been performed.

A total of 160 power supplies have been analysed. The results show that the SMPS topology used mainly depends on the SMPS operating power. Fig. 5 gives the repartition of the SMPS topologies for an output power range from 75 W to 150 W and 150 W to 1 kW.

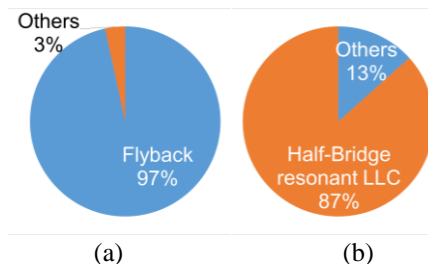


Fig. 5. (a) SMPS between 75 W and 150 W – (b) SMPS between 150 W and 1 kW.

Between 75 W and 150 W for SMPS output, a majority of flyback topology is present, while between 150 W and 1 kW, the half-bridge resonant LLC topology is mostly used.

Moreover, discussions with these PWM controller manufacturers permit to have another view which is that nowadays, with the power reduction trend, more and more SMPS based on flyback topology are used. This is confirmed by Fig. 6 showing that, without output power distinction, nearly 90 % of all studied SMPS use a flyback topology.

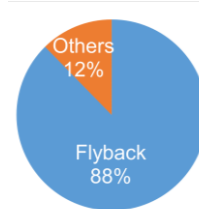


Fig. 6. Flyback topology proportion among the 160 studied SMPS.

Based on these results, a bunch of flyback SMPS of the same output power range, chosen among major manufacturers like Delta Electronics, Mean Well, Murata, TDK Lambda, etc. [12] was tested (up to destruction) with

PIC to verify their susceptibility. These first tests have shown that the same components are often destroyed like presented in Fig. 7.

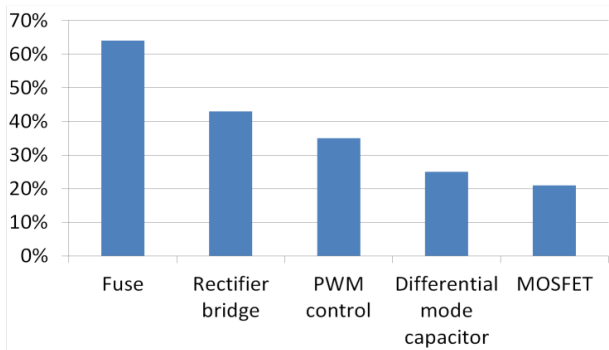


Fig. 7. Ratio of the different destroyed components.

In most cases, the fuse is destroyed. However, it is never the only failed component, meaning that its destruction is not directly caused by the injected current pulse but is the consequence of the destruction of another component. It is interesting to observe that mostly the input stage of the SMPS, including the differential capacitor, the rectifier bridge and the fuse, is damaged. It is quite logical, because it is the first stage to be “struck” by the injected current.

However, it can also be noticed that such an injection current can also destroy components placed deeper in the SMPS like the PWM control IC and the MOSFET transistor. Although destroyed SMPS use different topologies and components, the same components were often destroyed.

2.2.2. The designed SMPS for the study

Based on the SMPS topology analysis and the destruction results, a flyback SMPS, representative of a majority of current power supplies has been specially designed in order to facilitate destruction understanding. The electrical schematic of the SMPS is given in Fig. 8 and its picture is presented in Fig. 9. In order to perform several destructive tests, 100 SMPS samples were manufactured.



Fig. 9. Picture of the designed and tested SMPS.

During operation, the SMPS generates a 19 V output voltage and can supply a 3 A current, corresponding to a maximum operating power of 57 W, which classifies this SMPS in medium power range classically used for applications such as laptops, display screens, etc.

3. Destruction results

High current pulse injections have been carried out in common-mode and in differential-mode on 15 flyback power supplies (8 in common mode and 7 in differential mode). For this study, injection levels are progressively increased until reaching the Device Under Test (DUT) destruction threshold. Moreover, the interference pulse is injected when the main voltage is at its minimum value as shown in Fig. 10. The injection moment could be changed to study its effect but it is not considered in this study.

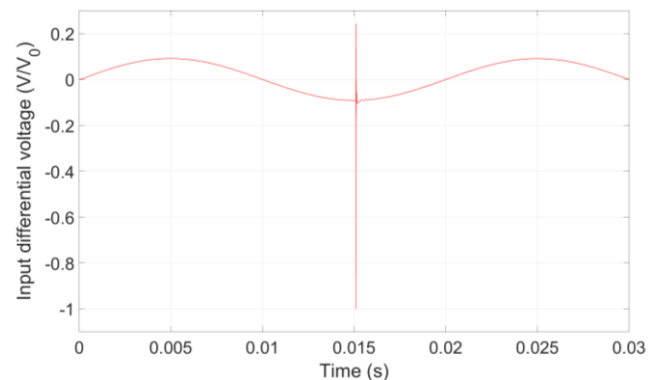


Fig. 10. Pulse synchronization with the main voltage.

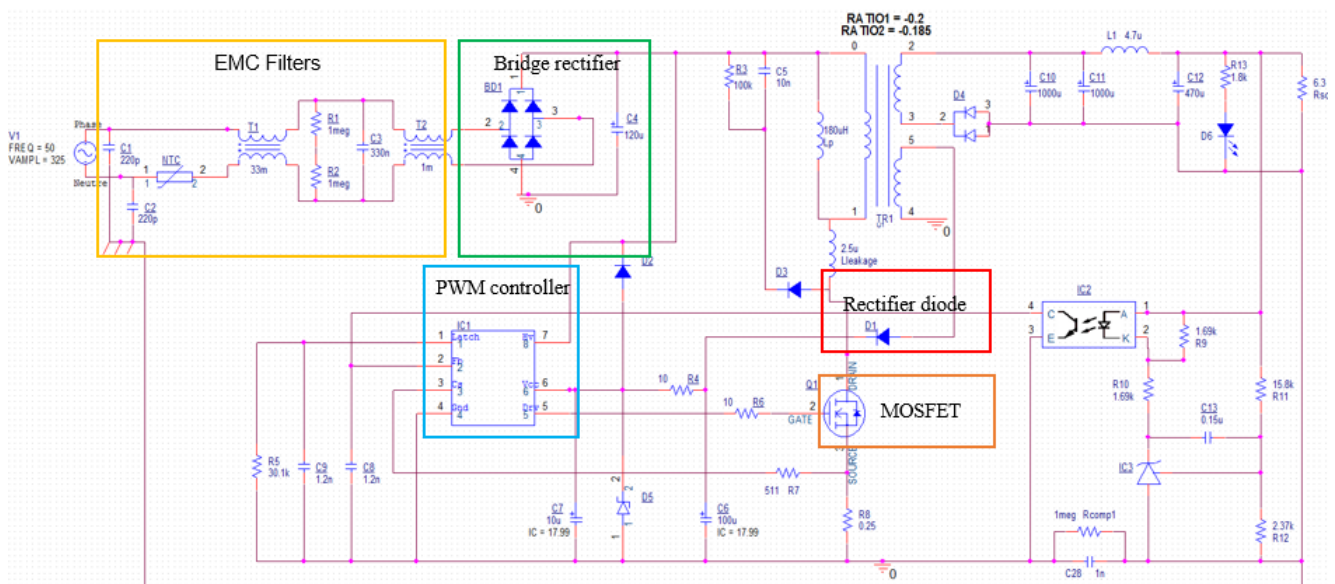


Fig. 8. Electronic schematic of the SMPS.

These tests permit to highlight two interesting conclusions:

- The first one concerns the destruction level needed to induce a failure in common mode and differential mode,
- The second one regards the components that have been destroyed in most cases.

3.1. Common mode and differential mode currents

All the 15 SMPS have been destroyed. After analysing all the input currents at the injection moment (common mode current or differential mode current) generating the failure, it seems that a lower current level is required in common mode to destroy the DUT than in differential mode. In fact, as shown in Fig. 11, measured destruction current level in common mode is about 40 % lower than the differential mode one. Therefore, SMPS are more susceptible in common-mode than in differential-mode. Such conclusion has also been obtained on similar injection study performed on power converters [7] but the reasons are not yet known.

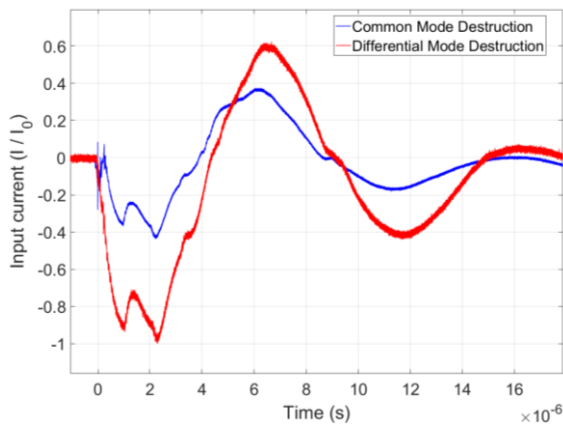


Fig. 11. Measured destructive input current in common mode and in differential mode.

3.2. Failed components

An analysis of the SMPS after failure has shown that, whatever the injection mode, most of the time, the same components were destroyed. Let's specify that there is, based on the today's investigation, no particular destruction mechanism identified related to one injection mode.

Moreover, destroyed components are overall the same ones as those of the commercial SMPS tested in the preliminary study.

Two main failure scenarios have been observed:

- 12 of the 15 SMPS have the D1 diode destroyed. As shown in Fig. 8, this diode is the rectifier diode on the PWM controller auxiliary supply.

- 3 of the 15 SMPS have the following failed components (see in Fig. 8): BD1 rectifier bridge, R6 resistor on the MOSFET gate, R8 shunt on the MOSFET source, Q1 MOSFET, D1 diode of the PWM controller supply and IC1 PWM controller.

4. Destroyed components analysis and understanding

4.1. Failure analysis

To understand the components destructions, X-ray, microscope and electrical analyses have been performed. X-rays and microscope allow to observe open-circuits, short-circuits or destroyed parts of components while electrical analyses allow to determine the electrical component behaviour once it has failed. The complementarity of these 3 techniques allow to propose some hypotheses to explain the component failure mechanisms. Note that for microscope analyses, the chip plastic packaging is firstly removed by acid attack before the chip can be observed with the optical microscope.

4.1.1 Rectifier diode

D1 is a MMSD914T1G diode from ON Semiconductor. X-ray analysis permits to observe in Fig. 12 a destroyed diode D1. In Fig. 12, the broken bonding wire is visible. Metal particles are spread around the bonding wire. In fact, the destruction of the bonding wire creates a conductive area close to it and, in this case, shorts the diode device. On other samples, only open circuit diode was observed.

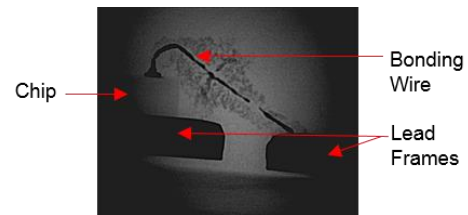


Fig. 12. Destroyed D1 diode.

Failure of diodes in power converters is relatively well documented. Some useful information can be found in [13, 14, 15]. Two main reasons can lead to the diode destruction. The first one is an overcurrent while the second one is an overvoltage.

Failure due to overvoltage is classically due to an avalanche effect. It is observed on a diode when the reverse voltage applied to diode terminals exceeds a specified value. This breakdown phenomenon usually causes a catastrophic failure shown in [13] for example. In fact, in devices with planar junction termination, the chip edge usually limits the maximal possible voltage blocking capability. So, avalanche breakdown first occurs at the chip edge. The occurrence of such a failure at this peculiar position indicates that the failure is caused by an overvoltage [16]. Failure caused by overcurrent is generally observed when the current exceeds the maximum value of the non-repetitive peak surge current given by the manufacturer. For example, usually, the overcurrent capability of a diode (during 1 ms) is 10 to 12 times the nominal current [16]. In our case, the X-rays picture presented in Fig. 12 and literature analysis suggest that the failure of D1 is probably due to a surge current. Moreover, D1 peak current measurement performed during pulse injection on SMPS supports this hypothesis, since the measured peak current was higher than the maximum surge current of 2 A specified in the datasheet.

4.1.2 Rectifier bridge

The rectifier bridge reference is UD4KB80 from Shindengen. In all failure cases, 2 diodes from the same diagonal are short-circuited. The goal of the X-ray analysis is to observe these short-circuits.

Fig. 13 presents an X-rays picture of one of the short-

circuited diode's junction. The picture shows a metal connection between two lead frames (red circle on the picture). The chip is the light grey part sandwiched between these two lead frames. Other views permit to see that this metal link is in parallel to the diode chip, short-circuiting the chip.

A milliohmeter measurement gives a resistance value of 11 mΩ.

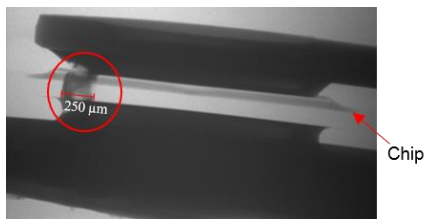


Fig. 13. One destroyed diode of the rectifier bride.

Based on the hypothesis described in 4.1.1, the short-circuit is most probably due to a high current [16] involving melting of the chip connections. Therefore, this melting creates a metal link in parallel to the chip. A high-current on bridge rectifier terminals is not surprising since several hundreds of amperes are injected at the SMPS input.

4.1.3 MOSFET

The MOSFET is a CoolMOS SPA11N65C3 from Infineon. Its technology owns a superjunction which offers low static and dynamic losses to increase switching efficiency.

The microscope analysis in Fig. 14 permits to show the MOSFET chip failure. In fact, the source failure with melted metal is visible. Moreover, a part of the passivation layer located on the MOSFET peripheral areas aiming to protect chip against the external environment is also destroyed.

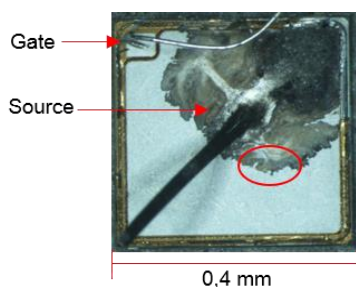


Fig. 14. Whole MOSFET microscope view.

According to the zoom of the destruction area presented in Fig. 15 and a SEM (Scanning Electron Microscope) analysis not presented here, the melted metal on the source part is, in fact, observed above the thin metallization layer of the source.

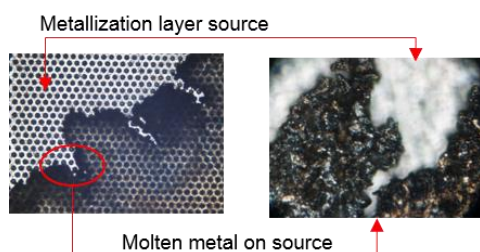


Fig. 15. Zoom of the MOSFET failure area.

These considerations (Fig. 14 and Fig. 15 microscope views and literature analysis [16, 17]) allow to suggest that the failure is due to a high current in the MOSFET which creates a peak power dissipation. This current density involves a temperature rise and produces a thermal runaway. During the MOSFET thermal runaway, periodical constraints of compression in the metallization layer are introduced due to the mismatch between the aluminium and the silicon expansion coefficients. The destruction damages the source metallization and can create a short-circuit between component terminals such as drain source and gate drain. Such an explanation is corroborated by electrical analyses which show that when the transistor fails, a short-circuit between drain and gate or source and gate is observed.

4.1.4 PWM controller

On the designed power supply, the PWM controller, which is the heart of the SMPS, is a NCP1271 controller from ON Semiconductor. An X-ray analysis presented in Fig. 16 allows to see the chip, the bonding wires, and lead frames.

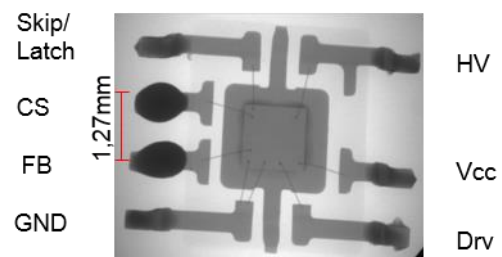


Fig. 16. NCP1271 X-ray analysis.

Since the X-ray analysis shows no defect, microscopy analysis has been undertaken. Fig. 17 shows a microscope view of the chip and its bonding wires.

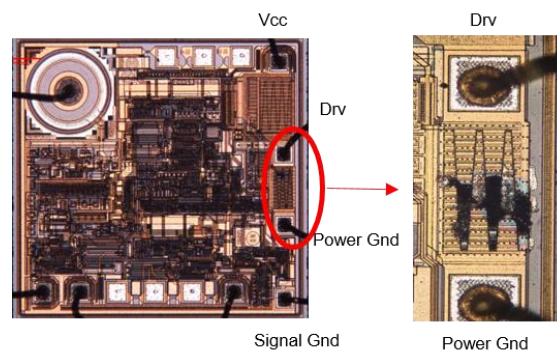


Fig. 17. NCP1271 microscope failure view.

Drv pin is the gate driver output including a high side switch (from Vcc to Drv) and a low side switch (from Drv to Power Gnd).

Right side of Fig. 17 is a zoom of the low side switch showing the destruction area. According to Fig. 16 and the visible melted metal, the destruction is probably due to a high-level current inducing a thermal runaway.

4.2 SMPS cascaded failures scenarios

The SMPS failure can be explained considering a high current injected into the rectifier bridge BD1, MOSFET Q1, shunt resistor R8, causing the destruction of these three components.

Additionally, if the MOSFET is short-circuited between gate and drain, a hypothesis would be that the MOSFET short-circuit allowed a current to flow through the gate external resistor R6, inside the controller Drv pin, then destroying the low side switch. Measurements must be performed to confirm this hypothesis.

Regarding the PWM controller auxiliary power supply, D1 diode failure is caused by an overcurrent.

A hypothesis would be that D1 diode fails because the PWM controller is disturbed during the injection, thus sinking a high transient current into its supply pins (Vcc or most likely HV). This current transient could be sufficient to destroy the diode D1.

Further investigations need to be performed to well understand the chronology of destruction events leading to the SPMS failure.

5. Conclusion

In this paper, a study of the effect of high-power pulse injection on a flyback power supplies has been presented. Many results have been obtained and some conclusions can be proposed. Firstly, it has been observed that, the destruction current average level in common mode injection is 40 % lower than the differential one. Moreover, it has been observed that globally four components of the SMPS were often destroyed during the pulse injection: the rectifier bridge, the PWM control, the MOSFET and the rectifier diode.

X-rays, microscope and electrical analyses have permitted to propose hypotheses for the component failure mechanisms. Moreover, studying the destruction cause of each failed components has also permitted to propose chronological sequence of destruction events explaining the SMPS failure.

Now, the aim will be to confirm these hypotheses. In order to perform such task, measurements of current and voltage waveforms during the flyback power supplies destruction will be undertaken at different locations of the SMPS. Studies on stand-alone components will be performed as well. Moreover, PSpice simulations of SMPS sections will help to understand the destruction mechanisms. The last step will be to model these destruction effects in order to be able to anticipate the irreversible effects that EMP could induce on electronic equipment.

Acknowledgements

This study has been carried out for Direction Générale de l'Armement (DGA).

Authors would thank very much B. Plano from IMS Laboratory who led X-ray and microscope analyses.

References

- [1] W. A. Radasky et al., "Brief historical review and bibliography for Intentional Electromagnetic Interference (IEMI)," XXXIth URSI General Assembly and Scientific Symposium, 2014.
- [2] R. Tcheumeleu Tientcheu et al., "Analysis of methods for classification of intentional electromagnetic environments," International Conference on Electromagnetics in Advanced Applications, 2015.
- [3] R. Montañó et al., "On the response and immunity of electric power infrastructures against IEMI – current Swedish initiatives," Asia-Pacific Symposium on Electromagnetic Compatibility, pp. 510-513, 2008.
- [4] D. Nitsch et al., "Susceptibility of some electronic equipment to HPEM threats," IEEE Transactions on Electromagnetic Compatibility, vol. 46, no. 3, pp. 380-389, 2004.
- [5] Y.V. Parfenov et al., "Conducted IEMI threats for commercial buildings," IEEE Transactions on Electromagnetic Compatibility, vol. 46, no. 3, pp. 404-411, 2004.
- [6] S. Lihua et al., "Experiments on the susceptibility of the direct digital control system to EMP in intelligent buildings," Asia-Pacific Conference on Environmental Electromagnetics, 2003.
- [7] M. L. Sudheer et al., "Study of conducted susceptibility of power converters," Proceedings of the International Conference on Electromagnetic Interference and Compatibility, 1999.
- [8] G. Mejezaze et al., "Common Mode Modelling of a Current Injection Source for Susceptibility Study," International Symposium on Electromagnetic Compatibility, pp. 833-838, Amsterdam, 2018.
- [9] S. James et al., "Investigation of failure patterns of desktop computer power supplies using a lightning surge simulator and the generation of a database for a comprehensive surge propagation study," Conference on IEEE Industrial Electronics Society, 2010.
- [10] M. Girard et al., "Effects of HPEM stress on GaAs low-noise amplifier from circuit to component scale," Microelectronics Reliability, vol. 88-90, pp. 914-919, 2018.
- [11] International Electrotechnical Commission – TC77/SC 77C, "Electromagnetic compatibility (EMC) - Part 2: Environment - Section 9: Description of HEMP environment - Radiated disturbance," IEC 61000-2-9, 1996.
- [12] Power & Energy service of IHS, "The World Market for AC-DC & DC-DC Merchant Power Supplier," 2013.
- [13] H. Egawa, "Avalanche characteristics and failure mechanism of high voltage diodes," IEEE Transactions on Electronic Devices, vol. 13, no. 11, pp. 754-758, 1966.
- [14] I. Dchar et al., "SiC power devices packaging with a short-circuit failure mode capability," Microelectronics Reliability, vol. 76-77pp. 400-404, 2017.
- [15] R. Wu and al., "Overview of catastrophic failures of freewheeling diodes in power electronic circuits," Microelectronics Reliability, vol. 53, no. 9-11, pp. 1788-1792, 2013.
- [16] J. Lutz and al., "Semiconductor Power Devices – Physics, Characteristics, Reliability," Springer, 2011.
- [17] F. Richardeau et al., "Gate leakage-current, damaged gate and open-circuit failure-mode of recent SiC Power Mosfet," IEEE International Conference on Electrical Systems for Aircraft, Railway, Ship Propulsion and Road Vehicles & International Transportation Electrification Conference, 2018.